Asociación Argentina
de Mecánica Computacional

Mecánica Computacional Vol XXXI, págs. 3693-3714 (artículo completo)
Alberto Cardona, Paul H. Kohan, Ricardo D. Quinteros, Mario A. Storti (Eds.)
Salta, Argentina, 13-16 Noviembre 2012

NUMERICAL AND EXPERIMENTAL EVALUATION OF SKIMMER TANK TECHNOLOGIES FOR GRAVITY SEPARATION OF OIL IN PRODUCED WATER

Damian E. Ramajo[a], Marcela Raviculé[b], Clarisa Mocciaro[b], Pablo Weismann[a] and Norberto M. Nigro[a]

[a]*International Center for Computational Methods in Engineering (CIMEC)*
INTEC-UNL-CONICET, Güemes 3450,S3000GLN Santa Fe, Argentina
dramajo@santafe-conicet.gov.ar

[b]*Centro de Tecnología Argentina (CTA), YPF, Baradero s/nro. 1925, Ensenada, Argentina*
mravicules@ypf.com

Keywords: CFD, measurement, skimmers, water/oil separation

Abstract. Computational Fluid Dynamics (CFD)and experimental tests were used to carry out a comparative study of gravity separation using skimmer tank technologies for removing low oil concentrations remaining in produced water. In this work, two technologies were evaluated; one without internals (called *descendent flow technology*) and the other with internals (called *baffle technology*). For experimental tests, a pilot tank of 2000 liters was built. The flow, residence time and canalization effects were evaluated by performing conductivity measurements, injecting a sodium chloride pulse at the inlet and measuring conductivity profile at the outlet. For the first technology (*descendent flow*) canalization was strong, and that was evidenced by several conductivity peaks a few minutes after salt injection (the mean theoretical residence time was 4 hours). On the other hand, for *baffle technology* only one conductivity peak was detected after 140 minutes, showing the much more volume efficiency of the tank.

At first, CFD validation of experimental data was performed by solving the advection-diffusion transport equation for salt concentration(eulerian strategy) over a steady state flow previously calculated for water. Although this methodology catches the first peak for the *descendent flow technology*, the subsequent peaks are not evidenced. For this reason, an alternative strategy (particle tracking) was used to represent salt flow, allowing to reproduce the full conductivity data profile and to estimate the mean residence time for both skimmer tanks.

Computational time was considerably reduced by the use of lagrangian strategy. Results from descendent flow technology were in good agreement with experimental data, leading to the conclusion that the implemented CFD strategies is suitable for evaluation and design of skimmer tanks with long residence time.

1. INTRODUCTION

Produced water quality has become an increasingly large area of concern for the oil production industry. Production facilities have been re-evaluating their conventional approaches to oil removal from water due to increasing water cuts caused by the maturation of their oil wells, as well as a need for cleaner water for re-injection or disposal purposes. As such, the main concerns for producers are that not only do many facilities require an upgrade to their existing equipment to handle higher capacities, but also that their facilities require a more rigorous, reliable system to maintain their water quality for re-injection or disposal specifications. Conventional approaches for water de-oiling include the use of equipment such as gravity skimmer tanks, CPI's, induced gas flotation units, hydrocyclones and filters. Skimmers have been used for a long time, because on their simplicity, low cost and low maintenance. Disposal piles and skimmer tanks can remove a minimum drop size ranging 100-150 μm (Stewart and Arnold, 2008; Trambouze, 2002). The function of this kind of equipmentis to cause the oil droplets, which are dispersed in the water continuous phase, to separate and float to the surface to be removed. The two basic phenomena that are involved in the design are settling and coalescence. The more recent technologies uses gas flotation for settling improvement (Man et al., 2005; Lee et al, 2007), but air pumps need maintenance and energy supply. Turbulence can disperse drops or caused emulsion so it must be avoided (Stewart and Arnold, 2008). Settling is relatively well described and understood in the context of Stoke's law: the smaller the droplets of the dispersed phase the more difficult phase separation becomes (Çengel and Turner, 2001). Coalescence is less well understood, as it is often driven by chemical interactions on interfaces of the dispersed droplets: bringing two droplets into contact does not automatically guarantee their coalescence (Billingham, 1992).
Skimmers require substantial retention time for acceptable performance and efficiency downs for heavy oil or emulsions loads. There has been a shift within the overall industry to improve the basic designs including internal structures or distribution nozzles to encourage the coalescence of oil droplets within the tank. Among those, include tangential nozzle entry to promote swirling and oil droplet coalescence along the sides of the tank (Stall, 1981), as well as internal baffles or small hydrocyclones within the tank. The inlet design become crucial to provide a more uniform flow on entry to the tanks (Lee and Frankiewicz, 2005). For example, momentum breakers such as impingement and baffle plates or turbine-vane arrangements are routinely installed in the separators (Zhang et al., 2007; Hansen, 2005; Wilkinson et al. 2000; Jeelani and Hartland, 1998).
The residence time distribution (RTD) is a concept which may be used to describe the flow behavior of the mixtures in the separator (Jaworski and Meng, 2005). Although the mean residence time (MRT) cannot be far from the theoretical residence time (TRT), the RTD is crucial to know the tank behavior (Simmons et al., 2002; Simmons et al., 2004). In this paper, numerical and experimental RTD are obtained for two typical skimmer tanks. For experimental data, a pilot plant facility was made and salinity pulse methodology was applied to know the RTD. As regards numerical data, CFD studies using scalar transport (euler-euler) and particle transport (euler-lagrangian) methods were performed. The minimum residence time, which is the elapsed time after the first particles (or the salinity pulse) was detected at the outlet.

2. Methodology

Different flow rates were studied; 300, 500 and 800 l/h, which correspond to theoretical residence times of 6.6, 4 and 2.5 hours. RTD data was obtained focusing at the elapsed time required to start to detect the conductivity pulse or the first particle, which is a clear indicator of canalization effects.

2.1. Experimental facility

Figure 1 shows a pilot scale tank used to measure residence time and separation efficiency for different skimmer tank configurations. The scaled 1:10 tank with four polycarbonate mirrors for visual inspection, 1.6 m diameter and 1.1 m height (2.2 m^3 capacity) was built of fiberglass to avoid corrosion damage caused by the salt injected in RTD measure. The aspect ratio is the same as the typical skimmers of 2000 m^3 capacity.

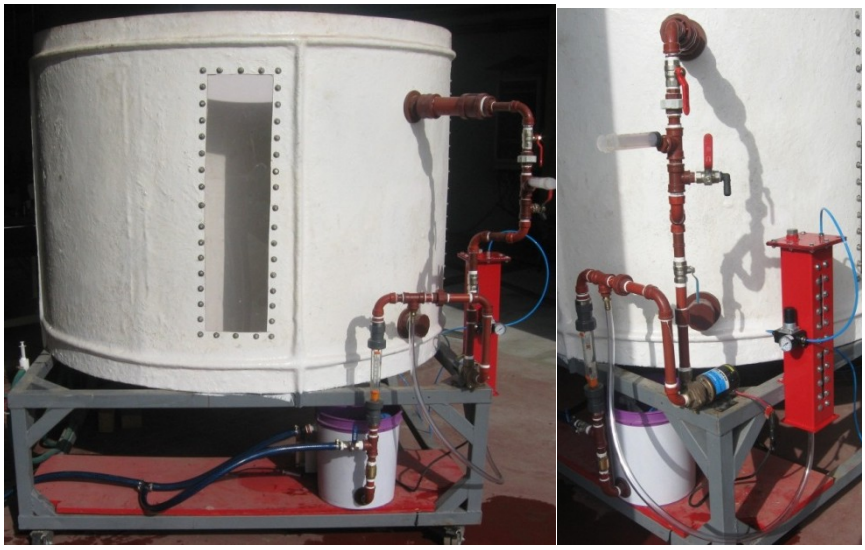

Figure 1: Pilot skimmer tank. View of the inlet system

The inlet system is composed of a 12 V CC centrifugal pump to induce water/oil mixing and to control the droplet size. The pump is feed with a stabilized CC electric supply (to control the pump speed). The flow is manually stabilized through valves and with the help of a flow meter (100 to 1000 l/h).The setup used to supply and control the oil injection can be observed in Figure 1.

Conductivity pulse measure: A saturated solution of sodium chloride in water is injected at the inlet through a 60 cm^3 syringe.

Oil measure: The oil is contained in a pressurized tank (red) which has a small orifice (2 mm) at the bottom. The oil is pushed by pressurized air from the top and flows through a hose towards the inlet system. The oil mass flow is controlled manually using a pressure meter ranging from 0 to 3 bar. The required oil flow is really low (less than 1 l/h) and corresponds to 800 ppm at the inlet. Once the oil and the water are put in contact they are mixed by the pump. The size of the oil droplets can be coarsely controlled by modifying the pump speed and closing the valve at the downstream of the pump.

Conductivity is measured by a conductimeter (Horiba ES-51) at the outlet system, and data is monitored and stored in a computer through on-line acquisition. Conductivity can be monitored both at the water (bottom) and the oil (top)outlet.

2.2. Computational simulation

In this work two type of tanks were studied:

1.-the descendent flow

a- it is the simplest one without inlet distributor (Figure 2 top, left)

b-with an inlet distributor made of a vertical tube with 12 holes (Figure 2 top, right)

c-with an inlet distributor made of a vertical tube with 30 holes (Figure 2 top, right)

2.- internal with vanes or baffles

a- with three vanes and a vertical inlet duct without holes (Figure 2 bottom, left)

b- with three vanes and a vertical inlet duct with four holes (Figure 2 bottom, right)

Note from Figure 2 that the skimmer 1b and 1c shared the same geometry and the holes were not included in it. In both cases the holes were represented through mass and momentum sources located at the surface of the vertical duct.

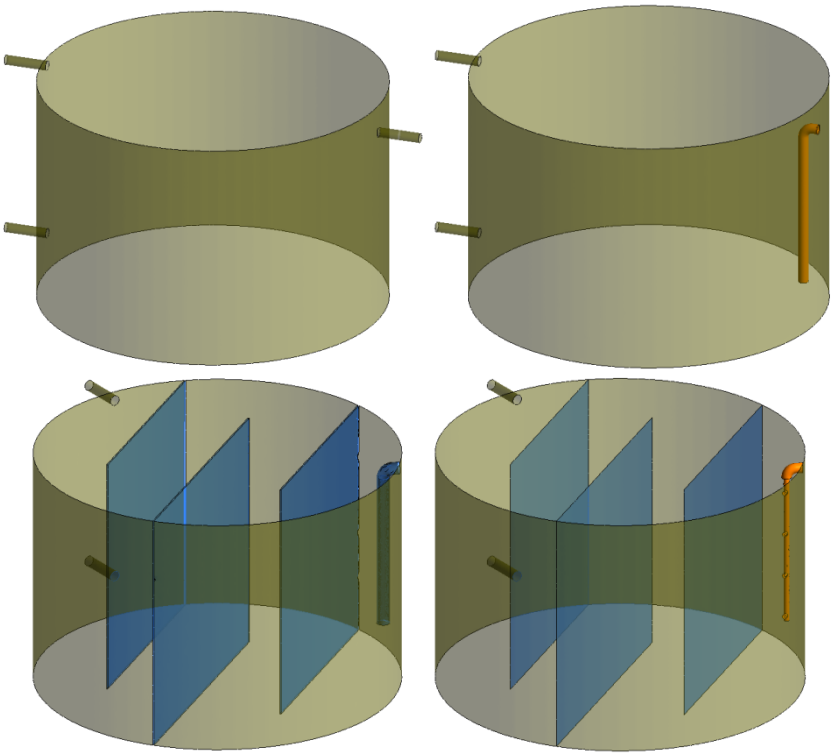

Figure 2:View of the four tanks analyzed. Upper, left: skimmer 1a. Upper, right: skimmer 1b and 1c. Bottom, left: skimmer 3a. Bottom, right: skimmer 3b

2.3 Governing equations

The water/oil mixture is a two phase system where small oil drops are immersed in a continuous liquid phase (water).

Continuous phase (water)

In this work only the continuous phase is initially solved using the one-phase Navier-Stokes equations for incompressible and isothermal flow. Once steady state is reached, the trajectory of the discrete phase (oil drops) is modeled through a lagrangian methodology.
For the continuous phase, turbulence is modeled through the Smagorinsky LES (Large Eddy Simulation) model.
For incompressible flow, the continuity equation is:

$$\nabla . u = 0 \tag{1}$$

where u is the Reynolds average mean velocity. Conservation of the momentum is given by:

$$\rho \frac{du}{dt} + \rho u . \nabla u = -\nabla P + \nabla . \left[(\mu + \mu_t)(\nabla u + \nabla u^T) \right] + \rho \vec{g} \tag{2}$$

In Eq. (2) the turbulent viscosity μ_t is modeled using LES Smagorinky model which solves for the flow eddies larger than the grid size and models the smaller ones assuming that $\mu_t = \mu_t = \mu_{SGS} \propto l q_{SGS}$. Then, the sub grid scale l is the length scale of the unresolved motion Usually the grid size $\Delta = V^{1/3}$, being V the volume of the cell. Finally q_{SGS} is the velocity of the unresolved motion.

$$\frac{\mu_t}{\rho} = (Cs\Delta)^2 \left| (\nabla u + \nabla u^T) \right| \tag{3}$$

In Eq. (3) the Smagorinsky constant for homogeneous turbulence is $Cs = 0.18$.
Equations were solved using the commercial package ANSYS CFX 13.0 (ANSYS, 2010) using distributed parallel computing facilities in a beowulf cluster of Intel(R) multiCore (TM) i7 CPU 950 3.07 GHz, 6 GB RAM.
Regarding time integration, due to LES requirement central difference was used for advection terms. A time step of $1x10^{-2}$ s was enough to obtain a *RMS* residual smaller than $1X10^{-6}$ for mass and momentum.

Discrete phase (Particle tracking)

Particle tracking was performed using an in-house particle tracking code (PTC) in C++ optimized for local parallel computing. The model is based on one-way interaction between the continuous and the discrete phase where the behavior of the continuous one is previously solved from any solver. The particle dynamic equation includes four forces terms: buoyancy, inertial, drag and added mass. Regarding turbulence, the PTC includes a random walk model based on the perturbation of the local position of the particles in function of the turbulence level associated to the turbulent viscosity ratio.
The temporal integration is carried out using a Runge-Kutta-Felhberg (RKF) integrator, and a novel analytical integrator is used to solve particle-wall collisions. Although ANSYS CFX has a particle transport model, it has two significant limitations. First, the random walk model is not enabled for LES turbulence model. Second, efficiency is poor and the computing time is around 30 times more than for the in-house PTC. Details about the PTC can be find in Gimenez et al (2012).

3. RESULTS AND DISCUSSION

3.1 Descendent flow skimmer (1a)

Figure 3 shows experimental data obtained for the simplest skimmer studied. Data correspond to a TRT of 4 hrs. Note that three main peaks are found. The first one appears for a elapsed time of only 150 s (2.3 min) and the others at 340 s (5.6 min) and 570 s (9.5 min), respectively. Separation between peaks is around 3.5 min. The first and second peaks are approximately the same size. The third one is 20% smaller than the others. In the same picture the numeric predictions based on particle tracking are drew. As noted, the first and second peaks are captured although the other seems not be represented by particles.

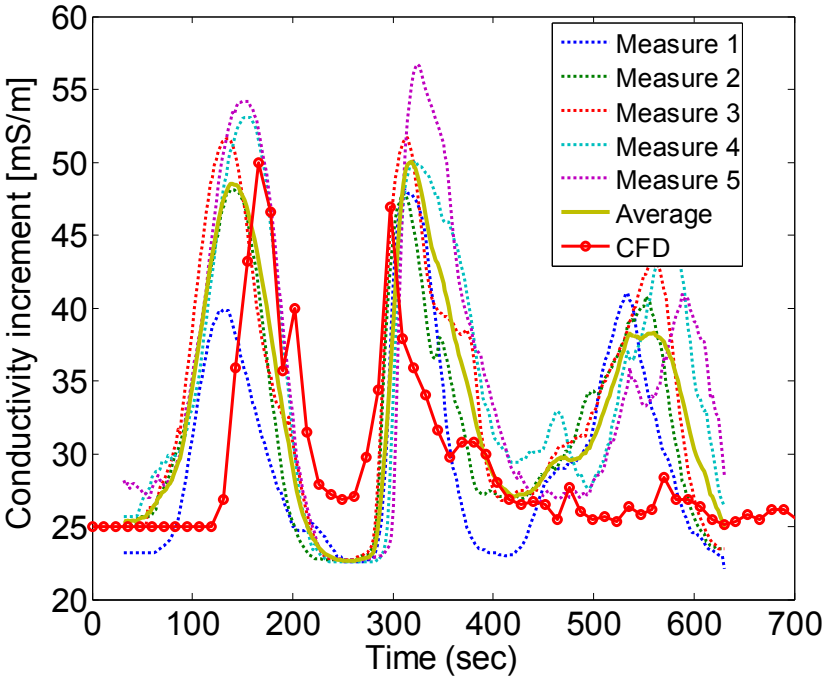

Figure 3: Experimental and numeric data comparison (TRT 4 hrs)

Figure 4 shows another model used for evaluating RTD. In this model the salinity pulse was represented as a scalar variable being transported through the steady state flow. Although this numerical strategy allowed to capture the first experimental peak, the others were not evidenced. Moreover, this type of calculus was strongly more time consuming than the particle tracking strategy. This can be explained because for the scalar transport method the variable concentration must be solved for all the mesh elements. On the other hand, particle tracking is locally solved for the elements where there are particles.

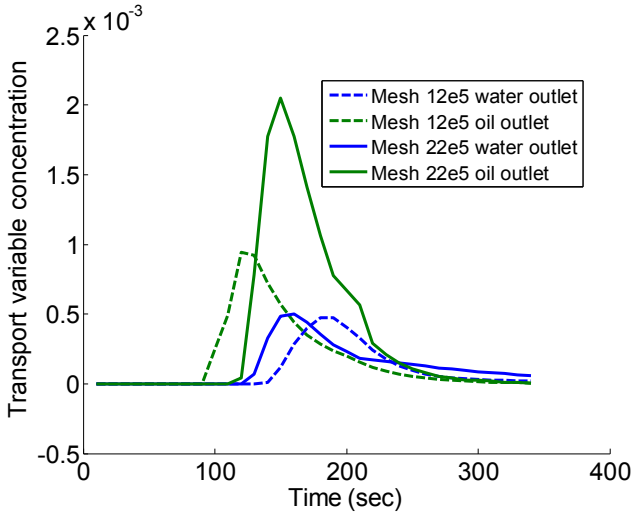

Figure 4: Saline pulse for oil outlet (oil, red curve) and water outlet (water, green curve)

Particles

Based on the fact that the advective transport of a concentration only allowed to capture the first experimental salinity pulse, a particle tracking strategy was implemented. The first steps were performed using the native CFX particle tracking model. Figure 5 shows results for the same two meshes. As noted, the finest mesh allowed to find the second peak experimentally observed. Particles start to leave the skimmer after a few seconds corresponding to a traveling length near 5 m.

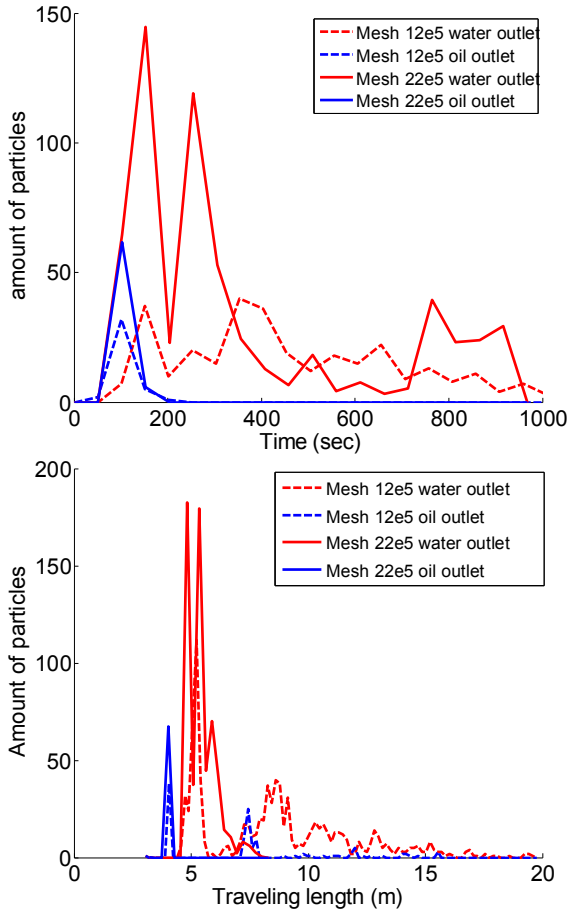

Figure 5: Results obtained using CFX particle tracking model. Left: amount of particles leaving the skimmer in the time. Right: traveling length

Visualization of the streamlines of the steady state flow can help to understand the existence of more than one peak on the RTD. Note that a large vortex structure is observed. Streamlines quickly travel from the inlet until the opposite wall skimmer and then descend and return to the inlet zone. In each "loop" the particles pass near the outlets and some of them leave the tank.

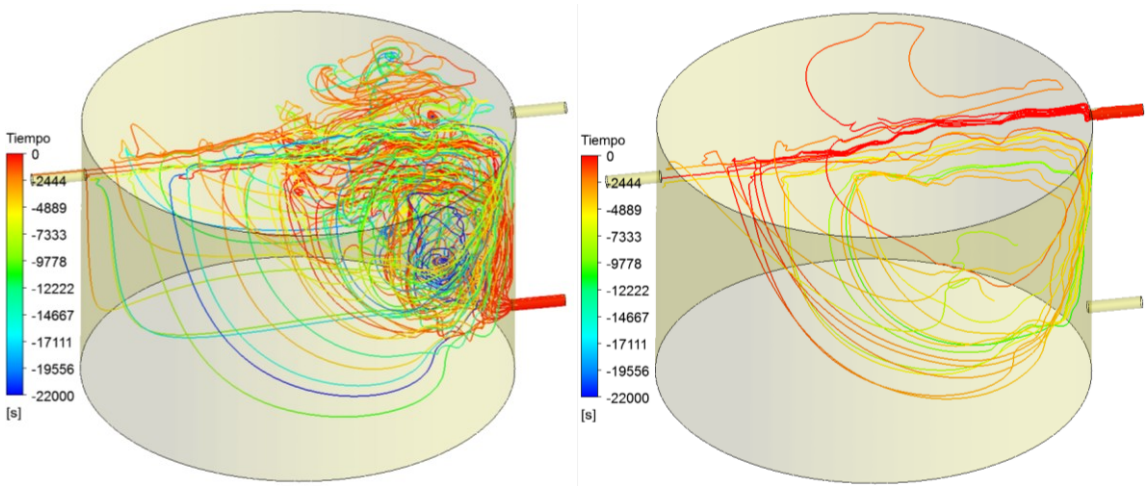

Figure 6: Streamlines starting from the inlet. Left: leaving the tank through the water outlet. Right: leaving the tank through the oil outlet

From the previous results, the numerical strategy based on particle tracking was adopted based on the best capture of results and the significant reduction on time computing. Results also allowing to define the mesh refinement required to capture the more significant flow structures.

Figure 6 shows the cumulative residence time distribution (CRTD) for a long time simulation (around 6 hours). Results corresponds to simulations using the in-hose PTC. Salinity pulse was represented by seeding 14700 particles at the inlet during the first 5 sec of the simulation. After 1000 s (16.6 min) 1845 particles leave the tank through the outlet at the bottom (water) and 207 particles through the outlet at the top (oil). As expected, the MRT defined by tracing a horizontal line at the 50% on the CRTD curve (Figure 7 at left) is not so far from the theoretical residence time (4 hours for this case). On the other hand, the CRTD is useful to quantify canalization effects. From this RTD results two conclusion can arise: first a high amount of particles quickly leave the tank (note that 10% of the particles resides less than 5 minutes) indicating canalization phenomena. Second, the time dispersion around the MRT is high.

Figure 7 at right shows the particle traveling lengths. Note that any of the particles leaves the tank until to travel for around 5 m. being the mean traveling length around 30 m.

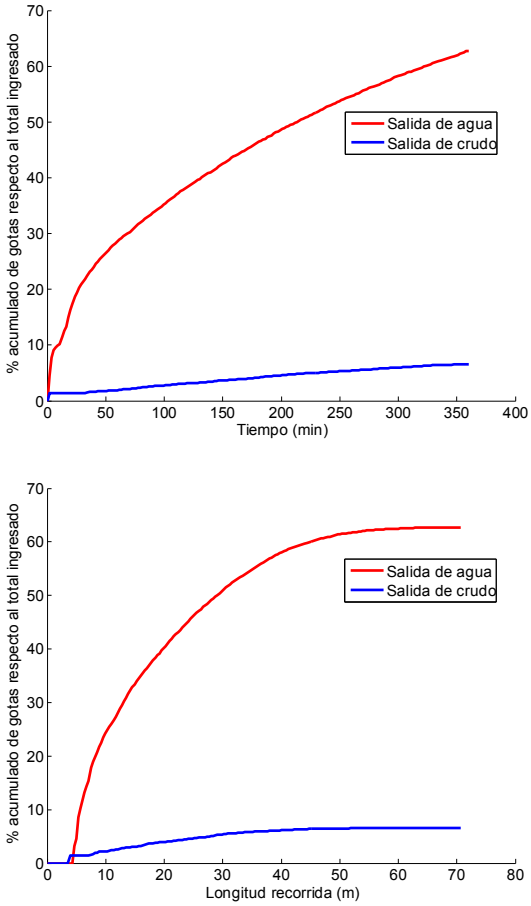

Figure 7: Cumulative percentage of particles leaving the domain. Left: as a function of time. Right: as a function of traveling length

Residence time distribution for oil drops

In this section results concerning to oil drops are presented. A parametric analysis considering two oil densities for light (900 kg/m^3) and heavy crude (930 kg/m^3) were performed. The separation efficiency as function of the drop size and the TRT was also investigated. Figure 8 at left shows the percentage of particles that leaves the domain through the water outlet (blue), the oil outlet (green) and reaching the free surface. Results corresponds to a 100 µm drop size. A drop that reach the free surface keeps until is captured for the collector tray, so the red and green curves can be assumed as the successfully separated curves. Figure 8 at left show the loose of efficiency caused for a reducing on the TRT. Note the strong increment on the amount of particles leaving the tank through the water outlet when TRT reduced from 4 to 2.5 hours. Figure 8 at right shows the effect on efficiency caused by the operation with different crudes (basically associated to a density change).

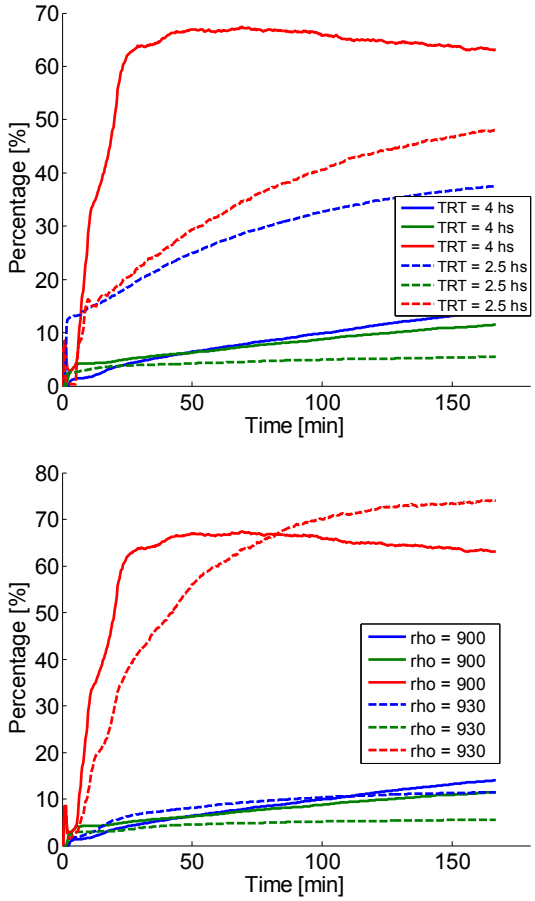

Figure 8: Skimmer 1a. Drop size: 100 µm. Left: for TRT of 2.5 and 4 hrs. Right: for TRT = 4 hrs and oil densities of 900 kg/m^3 and 930 kg/m^3

Figure 9 display the strong effect of the drop size on the separation efficiency. As expected, the more the drop size the best the separation. In this figure the red curves correspond to drops rising the free surface and blue curves correspond to drops leaving the tank through the water outlet. Results are in agreement with literature, showing the poor separation efficiency for particles with drop size of 50 µm. On the other hand, high efficiency is obtained for drop sizes greater than 100 µm.

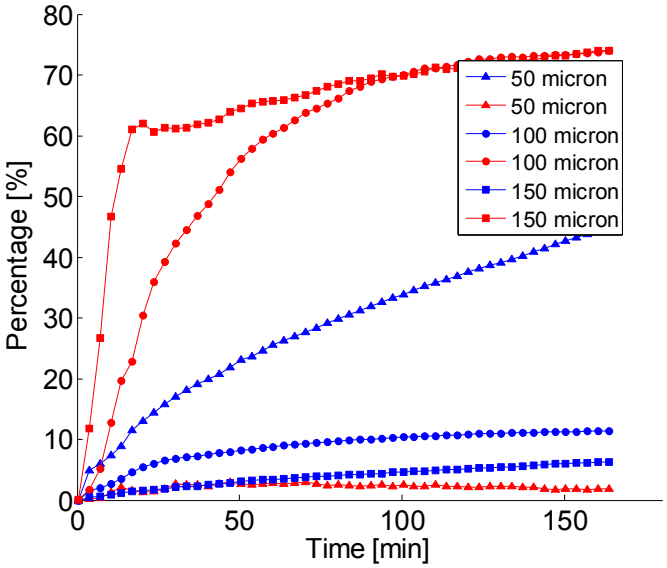

Figure 9: TRT 4 hours, oil density 930 kg/m^3. Particles leaving the domain through the water outlet (blue) and over the free surface (red)

In Figure 10 the instantaneous position of drops after 60 min of simulation is plotted using ParaView$^{(R)}$. As noted, for the smaller size (50 µm) the drops are almost homogeneously dispersed in the tank. On the other hand, 100 µm drops are more concentrated at the free surface. Finally, 150 µm drops the more of the drops are at the top of the tank.

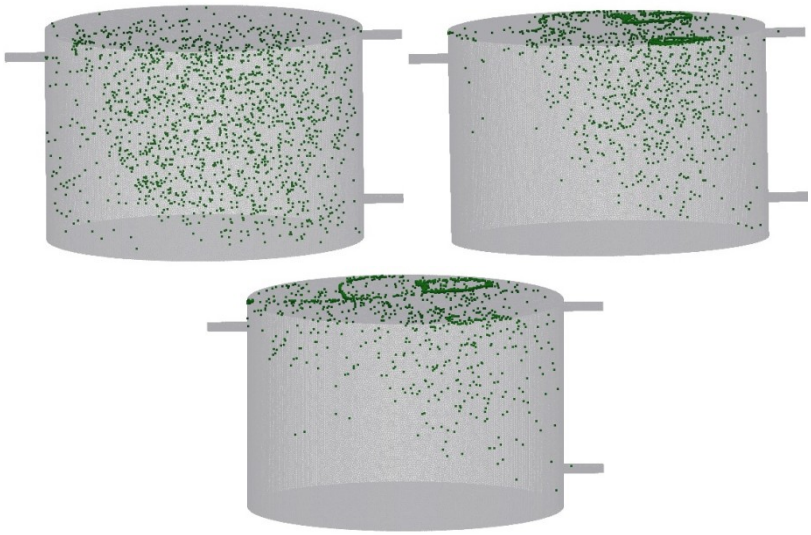

Figure 10: TRT 4 hours. Drops position (density 930 kg/m^3) after 60 min. Left: 50 µm. Center: 100 µm. Right: 150 µm

Figure 11 display the average drop height along the time for three drops sizes and non-buoyancy drops. Note that buoyancy effect is almost negligible for drops with 50 µm. The TRT have a significant effect on the drop location as noted by comparing the left and right

figures. For the TRT of 2.5 hours the results become closer and scarcely differences are found for 100 µm and 150 µm.

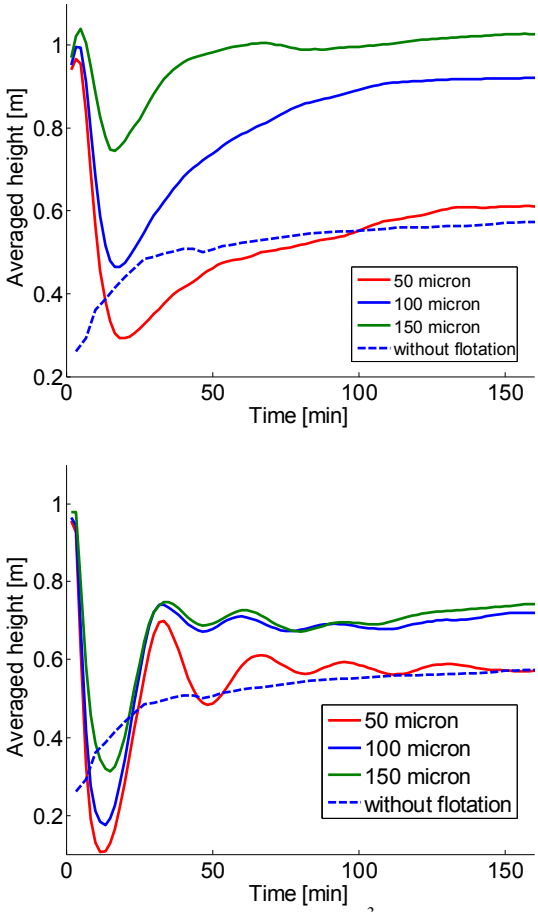

Figure 11: Average drop height (drop density of 900 kg/m^3). Left: TRT 4 hours. Right: TRT 2.5 hours

3.2 Descendent flow skimmers with inlet distributor with 12 (1b) and 30 holes (1c)

Figure 12 compares the results obtained by incorporating inlet flow distributors in order to improve flow homogeneity. Figure 12 at left corresponds to a drop size of 50 µm. Two effects can be clearly noted: first, the RT for the first particles to leave the tank be increased (around 10 min) for both distributor. Second, the amount of drops leaving the tank for the water inlet is significant reduced while the amount of drops rising the free surface is increased. Although these improvements are less significant for the 100 µm drops, for the 30 holes distributor the % of separation become closer to %95.

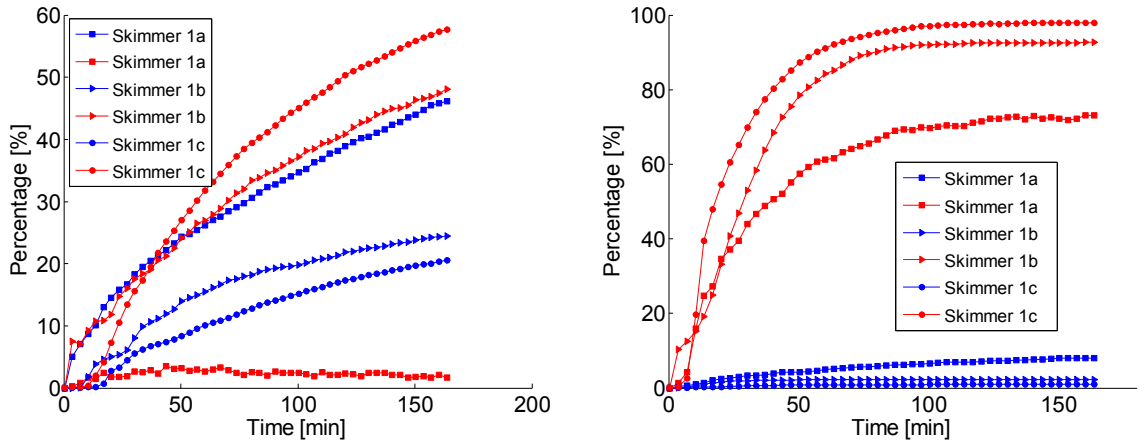

Figure 12: TRT 4 hours, oil density 900 kg/m^3. Particles leaving the domain through the water outlet (blue) and over the free surface (red). Left: drop size 50 µm. Right: drop size 100 µm

The average drops height showed in Figure 13 evidences the strongly improvement in performance for the smaller drops.

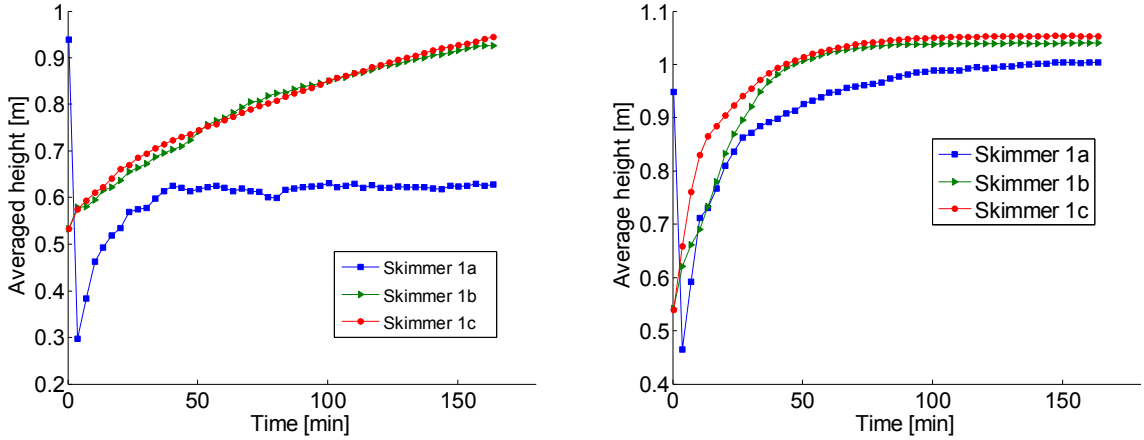

Figure 13: TRT 4 hours, oil density 900 kg/m^3. Average drops height. Left: drop size 50 µm. Right: drop size 100 µm

3.3 Skimmers with internals

Figure 14 displays the experimental results of salinity obtained for the internal skimmers 3a (Figure 14 at left) and 3b (Figure 14 at left). For the first one three TRT were measured while for the other one only the TRT of 2.5 hours was evaluated. Experimental data shows a reduction on canalization effects evidenced on the more time delay until the saline pulse start being measured. For TRT of 4 hrs this is around 25 min while for skimmer 1a was less than 2 min. For TRT of 2.5 hours the minimum residence time was of 12 min. Finally for a TRT of 6.6 hours this time was increased to 32 min. Different from previous case, the introduction of an inlet distributor with four holes (skimmer 3b) allowed to obtain a more typical RTD where distribution is dominated by a unique peak, quickly decaying. Although canalization is still evident, the peaks seems to be placed after one hour.

Saline pulse

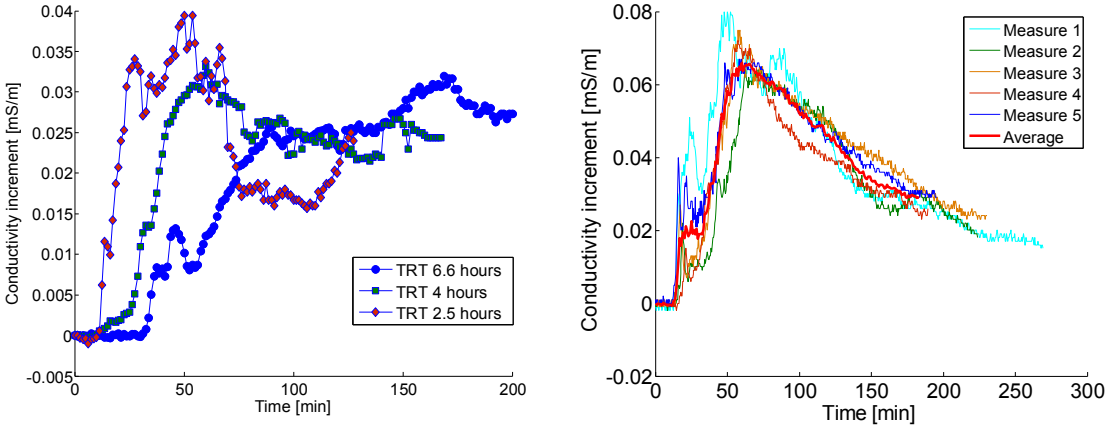

Figure 14: Sale pulse measurements for skimmer 3a. Average results over several measurements for three TRT

Visualization using a tracer

Flow pattern was studied qualitatively by injecting a pulse of a colored tracer (Rhodamine B) and taking pictures at different times. Figure 15 display a sequence of pictures from the upper for different times. Some interesting flow characteristics can be noted. For example, a large recirculation zone is evident where the tracer turn to the third compartment (around the vertex of the central intern).

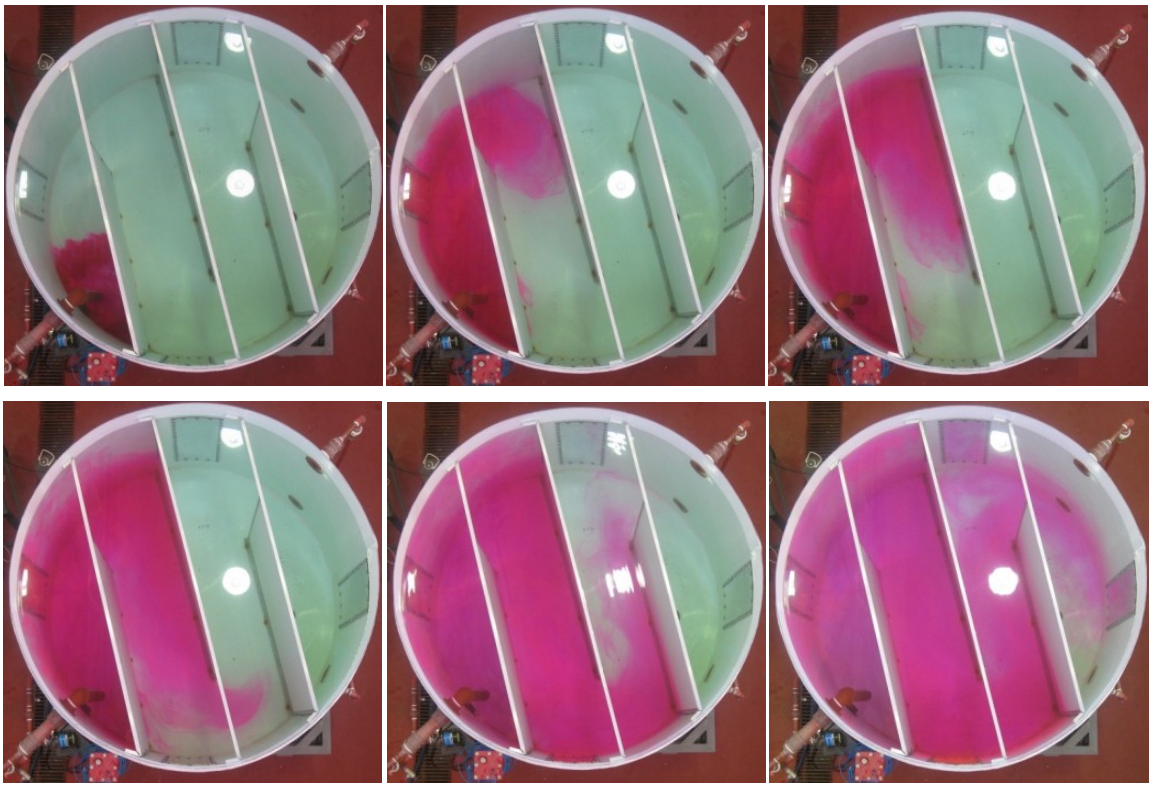

Figure 15: Upper view pictures of tracer for skimmer 3a (TRT 4 hours) for different times: 10 sec, 6 min, 9 min, 12 min, 18 min and 24 min

Figure 16 help to visualize the canalization phenomena. As noted, the tracer introduced at inlet travels through the bottom of the tank, filling less than a third part of the tank height. That could be the cause of the fast saline pulse detection at the outlet. The effect of the tank height on efficiency was not studied in this paper, but vertical stratification of the flow could be mitigated by employing a different aspect ratio. That will be analyzed in future work.

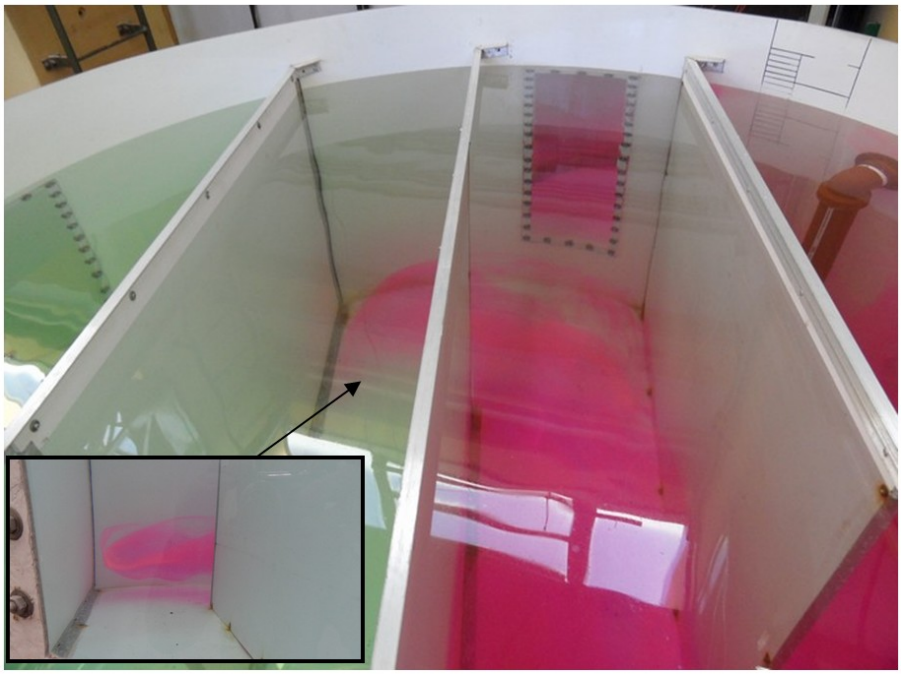

Figure 16: Tracer visualization for skimmer 3a (TRT 4 hours).

Regarding skimmer 3b, Figure 17 shows the inlet distributor. The picture at right shows how the tracer enters to the tank through four holes of equal dimension. CFD simulation shows that for this distributor the mass flow is not equal for all holes, being the percentage of the total mass flow from the upper to the lower hole are %15, %20,%30 and %35, respectively.
Tracer visualization shows complex vortex structures with high turbulence at the first tank compartment and re flow from the second to the first. As reported in Figure 14 at right, saline pulse is early detected around 15 min, and the conductivity peak appears around 50 min. CFD results are not in agreement with the first pulse detection.

Figure 17: Left: view of the four holes inlet distributor. Right: picture showing the tracer entering to the tank

Figure 18 shows the velocity field over four horizontal planes placed at the four inlet holes. For this tank the mesh was significantly refined in order to capture the complex turbulent structures. Results correspond to a mesh with 10e6 grid cells. In pictures only one of fifteen vectors was plotted. Some vortex structures are common along the planes, e.g. the big vortex at the beginning of the second compartment and the re-flow channel at the vertex of the first internal. Flow separation at the last vertex internal can be also found in all planes.
Figure 19 display a sequence particle locations for different times. Note that particles velocities are very intense along the first and second compartment of the tank. For the first four minutes simulation and experimental tracer data seems to be in good agreement. However, before entering to the third compartment the particles velocity become enough low (around 1 mm/sec).

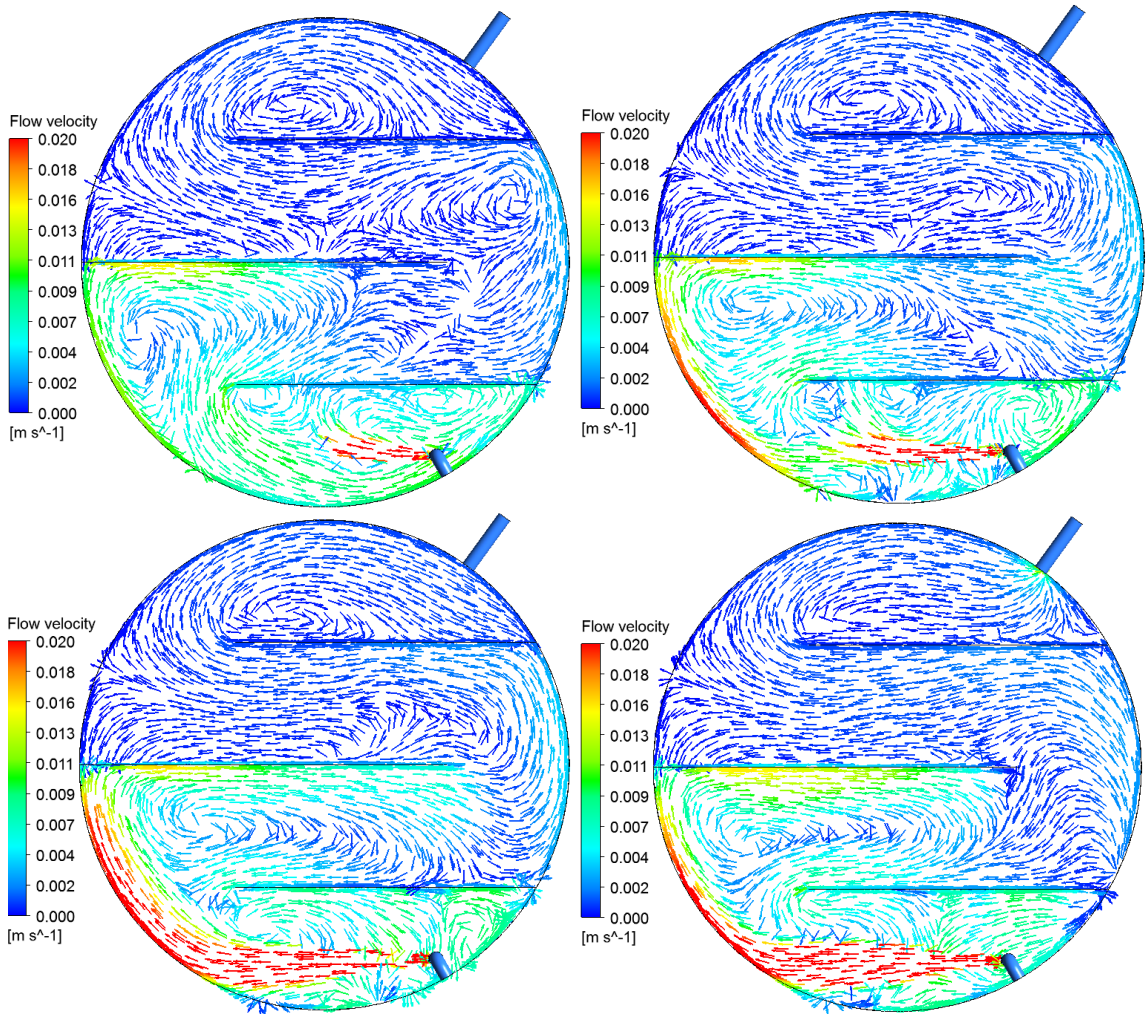

Figure 18: Velocity field over four horizontal planes placed at the four inlet holes Upper, left: first hole (0.82 m from the floor). Upper, right: second hole (0.627 m from the floor). Bottom, left: third hole (0.444 m from the floor). Bottom, right: four hole (0.24 m from the floor)

Figure 20 plots the amount of particles leaving the tank in time. as noted, they start to leaves after 36 min, while experimental data is around 16 min. However, the peak of particle outflow is similar for experimental and numerical data.

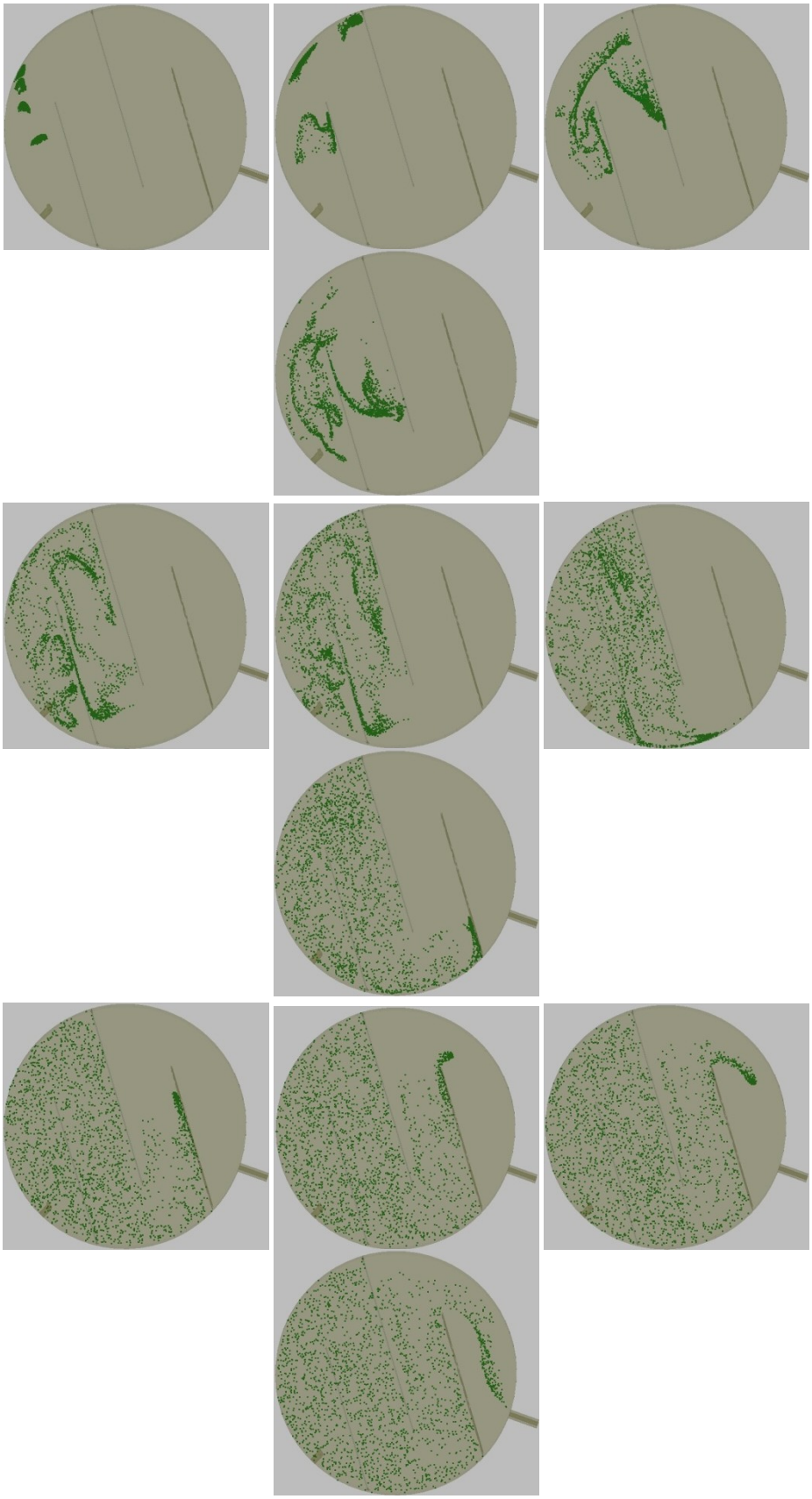

Figure 19: Particle positions for different times: 20 sec, 1 min, 2 min, 3 min, 4 min, 5 min, 8 min, 14 min, 20 min, 25 min, 30 min, 36 min

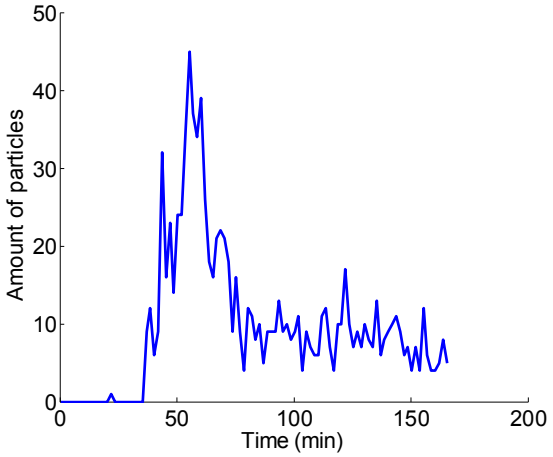

Figure 20: Skimmer 3b (TRT 2.5 hours). Amount of particles leaving the tank in time.

4 CONCLUSIONS AND FUTURE WORK

In this work numerical and experimental tests were performed over an in-house pilot skimmer tank facility. CFD results were in good agreement with experimental ones, although some calibration on turbulence modeling for particle tracking must to be done. However, the suitability of the numerical tools to study residence time and separation efficiency was assessed. Tests and tracer visualization shed light on some mean-flow characteristics that help to understand and verify the main vortex structures found by CFD. Based on these tests the following conclusions were reached:

1 - descendent flow skimmer has serious canalization problems that can be in part mitigated by introducing inlet flow distributors to reduce flow velocity.

2- the drop size seems to be the more relevant parameter for separation efficiency. The theoretical residence time (TRT) also have a crucial role and water density showed to be poor influence in separation performance.

3- CFD results were in concordance with literature showing that gravity-separation skimmers are not suitable for separating drops smaller than 100 μm

4- the introduction of internals increases the minimum residence time but are still far to remove canalization problems. Flow becomes very complex and turbulence play a crucial role on the prediction of the residence time distribution.

Future work will be devoted to improves the agreement between numerical and experimental results for internal tanks. Additionally, others technologies like vortex flow tanks and coalescence tanks will be studied both experimentally and numerically.

Glossary

CFD Computational fluid dynamics
PTC Particle tracking code
TRT Theoretical residence time
MFR Mass flow rate

RTD	Residence time distribution
MRT	Mean residence time
CRTD	Cumulative residence time distribution
u	Reynolds averaged velocity
t	Time
P	Pressure
ρ	Fluid density
Re	Reynolds number
μ	Viscosity
μ_t	Turbulent Eddy viscosity
μ_{SGS}	Subgrid-scale viscosity
l	Length scale of the unresolved motion in LES Smagorinky model
q_{SGS}	Velocity of the unresolved motion in LES Smagorinky model
C_S	Smagorinsky constant for homogeneous turbulence
CPI	Corrugated Plate Interceptors

Acknowledgements

Authors want to thank to CONICET, Universidad Nacional del Litoral and ANPCyT (grants PICT 1645 BID(2008), CAI+D 65-333 (2009)). They are also grateful to YPF for the support and interest.

REFERENCES

ANSYS.ANSYS CFX-Solver Theory Guide, 13th edition, ANSYS Inc., 2010.

Gimenez J., Ramajo D., Nigro N., Particle Transport in Laminar/Turbulent Flows. MECOM 2012, **Salta, Argentina, 2012.**

Jaworski A.J., Meng G., On-line measurement of separation dynamics in primary gas/oil/water separators: Challenges and technical solutions—A review, *Journal of Petroleum Science and Engineering***, 68, 47-59, 2005.**

Jeelani S. A. K. and Hartland S., Effect of Dispersion Properties on the Separation of Batch Liquid-Liquid Dispersions, *Ind. Eng. Chem. Res***, 37, 547-554, 1998.**

Kang W, Guo L., Fan H., Meng L., Li Y., 2011, Flocculation, coalescence and migration of dispersed phase droplets and oil-water separation in heavy emulsion, Journal of Petroleum Science and Engineering, 81, 177-181.

Lee C., Frankiewicz T., The Design of Large Diameter Skim Tanks Using Computational Fluid Dynamics (CFD) For Maximum Oil Removal, *15th Annual Produced Water Seminar***, Houston, USA, 2005.**

Man F., Owens N., Lee D., Rodriguez W., Induced Gas Flotation (IGF) within an API Skim Tank – A Case Study of Design Approach and Results, *GLR Solutions***, 2005.**

Lee D. W., Bateman W.J.D, Owens N., 2007, Efficiency of Oil/Water Separation Controlled by Gas Bubble Size and Fluid Dynamics within the Separation Vessel, *GLR Solutions,* **Calgary, Canada, 2007.**

Stall J.C., A Vortex Flow Water Settling System, *Amoco Production Company*, **Tulsa, 1981.**

Simmons M.J.H., Wilson J.A. and Azzopardi B.J., Interpretation of the flow characteristics of a primary–oil–water separator from the residence time distribution, *Trans IChemE, Part A, Chemical Engineering Research and Design*,**80(A): 471–481, 2002.**

Simmons M.J.H., Komonibo E., Azzopardi B.J., Dick D.R., Residence Time Distributions and Flow Behaviour within Primary Crude Oil–Water Separators Treating well-head Fluids, *Trans IChemE, Part A, Chemical Engineering Research and Design*, **82(A10): 1383–1390, 2004.**

Stewart M., Arnold K., Emulsions and Oil Treating Equipment, *Elsevier*, **2008.**

Trambouze P., 2000, Petroleum Refining: Materials and Equipment. *Institut Francais du Petrole Publication, Editions Technip*, **2000.**

Wilkinson D., Waldie B., Mohamad M. I., Lee H. Y., 1999, Baffle plate configurations to enhance separation in horizontal primary separators. Short communication. Chemical Engineering Journal, 77, 221-226.

Zhang L., Xiao H., Zhang H., Xu L., Optimal design of a novel oil-water separator for raw oil produced from ASP flooding, *Journal of Petroleum Science and Engineering*, **59, 213-218, 2007.**